Pro-inflammatory effects of human apatite crystals extracted from patients suffering from calcific tendinopathy.

Julien Herman
CHU Nantes: Centre Hospitalier Universitaire de Nantes
Benoit Le Goff
CHU Nantes: Centre Hospitalier Universitaire de Nantes
Julien De Lima
University of Nantes Faculty of Medicine: Universite de Nantes Faculte de Medicine
Régis Brion
University of Nantes Faculty of Medicine: Universite de Nantes Faculte de Medicine
Catherine Chevalier
University of Nantes Faculty of Medicine: Universite de Nantes Faculte de Medicine
Frédéric Blanchard
University of Nantes Faculty of Medicine: Universite de Nantes Faculte de Medicine
Christelle Darrieutort-Laffite (christelle.darrieutort@univ-nantes.fr)
Centre Hospitalier Universitaire de Nantes https://orcid.org/0000-0002-1871-0073

Research article

Keywords: apatite, rotator cuff tendons, interleukin-1, inflammasome, air pouch model

Posted Date: January 29th, 2021

DOI: https://doi.org/10.21203/rs.3.rs-156807/v1

Pro-inflammatory effects of human apatite crystals extracted from patients suffering from calcific tendinopathy.

Julien Herman (1,2), Benoit Le Goff (1,2), Julien De Lima (1), Régis Brion (1,3), Catherine Chevalier (1), Frédéric Blanchard (1)*, Christelle Darrieutort-Laffite (1,2)*

(1) INSERM UMR1238, Bone Sarcoma and remodeling of calcified tissues, Nantes University, 44035 Nantes, France
(2) Rheumatology department, Nantes University Hospital, 44093 Nantes, France
(3) Nantes University Hospital, 44093 Nantes, France

*Co-senior authors

Corresponding author:

Christelle Darrieutort-Laffite

INSERM UMR1238

Faculté de Médecine de Nantes

1 rue Gaston Veil

44035 Nantes cedex 1-France

E-mail : christelle.darrieutort@univ-nantes.fr

Tel : (+33) 240412895

Current address: McKay Orthopedic Research Laboratory, University of Pennsylvania, 307A Stemmler Hall, 3450 Hamilton Walk, Philadelphia, PA 19104-6081. Phone: 215-898-8653

Abstract

Background: Calcific tendonitis of the rotator cuff is due to carbonated apatite deposits in the shoulder tendons. During the evolution of the disease, an acute inflammatory episode may occur leading to the disappearance of the calcification. Although hydroxyapatite crystals-induced inflammation has been previously studied with synthetic crystals, no data are available with calcifications extracted from patients suffering from calcific tendinopathy. The objective of the study was to explore the inflammatory properties of human calcifications and the pathways involved.

Methods: Human calcifications and synthetic hydroxyapatite were used *in vitro* to stimulate human monocytes and macrophages, the human myeloid cell line THP-1 and human tenocytes. The release of IL-1β, IL-6 and IL-8 by cells was quantified by ELISA. Gene expression of pro- and anti-inflammatory cytokines was evaluated by quantitative PCR. NF-kB activation and NLRP3 involvement was assessed in THP-1 cells using a NF-kB inhibitor and a Caspase 1 inhibitor. The inflammatory properties were then assessed *in vivo* using a mouse air pouch model.

Results: Human calcifications were able to induce a significant release of IL-1β when incubated with monocytes, macrophages and THP-1 only if they were first primed with LPS (monocytes and macrophages) or PMA (THP-1). Stimulation of THP-1 by human calcifications led to similar levels of IL-1β when compared to synthetic hydroxyapatite although these levels were significantly inferior in monocytes and macrophages. Patient's crystals enhanced mRNA expression of *pro-IL-1β*, as well as *IL-18*, *NF-kB* and *TGFβ* when *IL-6* and *TNFα* expression were not. IL-1β production was reduced by the inhibition of Caspase 1 indicating the role of NLRP3 inflammasome. *In vivo,* injection of human calcifications or synthetic hydroxyapatite in air pouch led to significant increase in membrane thickness although significant overexpression of IL-1β was only observed for synthetic hydroxyapatite.

Conclusions: As synthetic hydroxyapatite, human calcifications were able to induce an inflammatory response resulting in the production of IL-1β after NF-kB activation and through NLRP3 inflammasome. In some experiments, IL-1β induction was lower with human calcifications compared to synthetic apatite. Differences in size, shape and protein content may explain this observation.

Keywords: apatite, rotator cuff tendons, interleukin-1, inflammasome, air pouch model

Background

Calcific tendonitis of the rotator cuff is due to carbonated apatite deposits in the shoulder tendons. It is a frequent cause of shoulder pain as calcific deposits are found in 10 to 42% of chronic painful shoulders [1]. Pain experienced by patients suffering from calcific tendonitis can affect their work life and daily activities. Calcific deposits appear between the tendon fibers after the formation of a fibrocartilaginous metaplasia containing chondrocyte-like cells [2]. These cells, derived from tenocytes, are able to mineralize the matrix through the action of alkaline phosphatase [3]. During the evolution of the disease, an acute inflammatory episode may occur leading to the disappearance of the calcification. This episode is characterized by rapid onset of severe pain and restriction of motion of the affected joint. The release of crystals in the subacromial bursa causes an acute bursitis responsible of this acute clinical presentation. Histological studies of calcific tendonitis have shown macrophages and multinucleated cells around broken-up calcium deposits, this would suggest their involvement in the initiation of the resorptive phase [4, 5]. Indeed, these macrophages contained mineral [5] and the multinucleated giant osteoclast-like cells expressed TRAP (Tartrate-resistant acid phosphatase) and cathepsin K, both involved in bone resorption [6].

Hydroxyapatite crystals-induced inflammation has been previously studied: *in vitro* and *in vivo*, synthetic hydroxyapatite was able to induce IL-1β and IL-18 release via the activation of the NLRP3 (NOD-like receptor family, pyrin domain containing 3) inflammasome [7-10] although TNF (tumor necrosing factor) seemed not to be implicated in this inflammatory response. In general, microcrystals like apatite, calcium pyrophosphate dihydrate (CPPD) or monosodium urate (MSU) crystals induce an acute inflammatory reaction mainly orchestrated by IL-1β. After crystal contact and detection by macrophages, IL-1β production and release occur (1) through NF-κB (Nuclear factor-kappa B) activation necessary for pro-IL-1β production and (2) through NLRP3 and caspase-1 activation to cleave pro-IL-1β into mature IL-1β. It is then released into the extracellular environment through damaged membranes of dying macrophages [11-12]. However, in all these data, authors used synthetic crystals and there is no data about the proinflammatory effects induced by carbonated apatite crystals extracted from patients suffering from calcific tendinopathy. Yet, human calcifications may differ from synthetic apatite through different particle size, shape and a rich protein content comprising most notably several proteins implicated in immune regulation such as Osteopontin [3,13]. It is not known if these

components could influence the inflammatory response induced by crystals. Since calcifications from patients differ from synthetic apatite, the objective of the study was to assess the pro-inflammatory effects of patients' crystals by studying synthesis of pro-inflammatory cytokines, in particular IL-1β, and the underlying mechanisms, focusing on NF-κB and NLRP3 inflammasome activation.

Methods

Crystal preparation

Human crystals from calcific tendonitis were collected from symptomatic patients by ultrasound-guided needle lavage and stored in PBS (phosphate buffered saline) at -80°C as previously described [3]. All patients enrolled gave their formal consent. Synthetic hydroxyapatite crystals (sHA) (REF-289396, Millipore Sigma, Switzerland) were first crushed using a mortar and pestle to obtain a powder close to the human crystals. Scanning Electron Microscopy was performed with a TM300 microscope (Hitachi, Japan) for further characterization. Human crystals and synthetic hydroxyapatite were diluted and dispersed by brief sonication in serum-free medium for *in vitro* experiments, and in PBS for *in vivo* experiments.

Cells

Human monocytic leukemia cells (THP-1, American Type Culture Collection, USA) were cultured in RPMI medium (Eurobio, France) with 10% of FBS (Fetal Bovin Serum, ThermoScientific, USA) and 1% penicillin/streptomycin (Lonza, Suisse). They were primed for 6 h with phorbol 12-myristate 13-acetate (PMA, 0.5µM, Sigma-Aldrich, USA), washed with PBS twice, then plated in 96-well plates at 50,000 cells/well and left overnight in complete media before crystal stimulation as described previously [11].

Peripheral blood CD14+ cells were extracted from healthy donors' samples. Peripheral blood mononuclear cells were isolated from blood samples obtained from the “Etablissement Français du Sang” by centrifugation over Ficoll gradient (Sigma-Aldrich). CD14+ cells were magnetically labeled with CD14 microbeads and positively selected by MACS technology (Miltenyi Biotec, Germany). CD14+ cells were CD3- by flow cytometry (purity ≥ 95%). For the experiments using monocytes, cells were plated (50 000 cells/well, 96-well plates) in αMEM medium (Thermofisher) with 10% FBS and 1% of penicillin/streptomycin. For macrophages, monocyte cells were incubated in GM-CSF (Granulocyte-Macrophage Colony Stimulating Factor) (25 ng/ml) and IFN-γ (Interferon gamma) (50 ng/ml) during 96h, or in M-CSF (Macrophage Colony Stimulating Factor) (25 ng/ml) during 72h (all from R&D systems, USA). All cells (monocytes or macrophages) were then washed once with PBS and were stimulated or not with LPS (lipopolysaccharide) (Sigma-Aldrich) at 0,1 µM overnight and washed with PBS twice before crystal stimulation [7].

Tenocyte-like cells were extracted from rotator cuff tendons as previously described [3]. They were plated in RPMI medium with 10% of FBS (5000 cells/well, 96-wellplate) and primed by LPS at 1µg/ml overnight then washed with PBS twice before crystal stimulation.

Primed THP-1, monocytes, macrophages and tenocytes were stimulated at the indicated times with human calcifications or synthetic apatite in FBS-free medium. For some experiments, THP-1 cells were incubated with an inhibitor of NF-kB (BAY-11-7085, 10µM, Sigma-Aldrich), or an inhibitor of Caspase-1 (Z-YVAD-FMK, 10 µM, Sigma-Aldrich) 30 minutes before crystal stimulation. After crystal stimulation, supernatants were collected for cytokine quantification and cells were analyzed for viability assay (WST-1, Takara Bio, France), protein expression or gene expression.

Air pouch model

Animal experiments were carried out in accordance with institutional guidelines and were approved by the French ethical committee CEEA Pays de la Loire and by local veterinary services (Approval number APAFIS#4969-2016041411376797v3). Seven-weeks-old female BALB/c mice and C57BL/6 mice (Janvier Labs, France) were used in the experiments. Mice were housed under standards conditions. Subcutaneous air-pouch were created by injecting 3 ml (day 0) and 2 ml (day 3) of sterile air into the dorsal skin of the mice under isoflurane anesthesia. At day 7, crystals prepared as described above were diluted in 1 ml of sterile PBS and injected in the air-pouch of the anesthetized mice. After 6 and 24 hours, mice were sacrificed, and membranes of the air-pouch were dissected. For each mouse, part of the membrane was fixed for histology and immunohistochemistry and the other part was dry frozen in liquid nitrogen for gene expression quantification.

Cytokine Quantification

ELISA kits for IL-1β, IL-6, IL-8 (R&D systems) were used for cytokine quantification in supernatants.

Reverse transcription-polymerase chain reaction (RT-PCR)

THP-1 total RNA was extracted using the NucleoSpin RNA Plus kit (Macherey-Nagel, Germany) while air pouch membranes total RNA was extracted using the NucleoSpin Set for NucleoZOL (Macherey-Nagel) after Turrax crushing.

First-strand cDNA was synthesized from 1 µg total RNA using the Maxima H Minus First Strand cDNA Synthesis Kit (ThermoScientific). Quantitative PCR was performed using SYBR Select Master Mix (Applied Biosystems, USA) and carried out on a CFX96 Real-Time PCR Detection System (Bio-Rad, USA). Primers used are reported in Supplementary Table 1. Resultant cycle threshold (Ct) values were normalized to the invariant control, HPRT (hypoxanthine-guanine phosphoribosyl transferase), and expressed as $2^{-\Delta Ct}$.

Western Blot Analysis

After 6 hours of crystal stimulation, THP-1 cells were lysed 15 minutes with Radioimmunoprecipitation Assay buffer containing protease inhibitors (Sigma-Aldrich), phenylmethylsulphonyl fluoride and orthovanadate (Sigma, Germany), on ice. Lysates were centrifuged and total protein concentration was determined by Bicinchoninic Acid Assay. An amount of 17 µg protein was separated in SDS-PAGE and transferred to PVDF (polyvinylidene fluoride) membranes for immunoblot analysis. Anti-NLRP3, IL-1β, cleaved-IL-1β and GAPDH (Glyceraldehyde 3-phosphate dehydrogenase) rabbit antibodies (Cell Signaling Technology, USA) were diluted at 1/1000.

Histology and immunohistochemistry (IHC)

Air pouch membranes were fixed in formol 4% during 24 hours before dehydration and paraffin-embedding. Three µm-thick sections were stained with hematoxylin and eosin (H&E). Membrane thickness was measured on H&E samples. The average of the thickness on 3 separate slides was calculated for each mouse. For IHC, sections were incubated with primary antibodies targeting Iba1 to identify macrophages (ab5076, Abcam, United Kingdom), Ly6G to identify neutrophils (ab25377,

Abcam), CD3 to identify T lymphocytes (ab5690, Abcam) and CD45R/B220+ for B lymphocytes (550286, BD Pharmingen, USA). Secondary antibodies were incubated at 1:400 for 2 h and streptavidin-HRP (P0397, Dako, USA) was incubated for 1 h, both at room temperature. Staining was achieved with DAB (TA-125-QHDX, ThermoScientific) and counterstaining was performed with hematoxylin. Cells were considered positive when stained in brown. Brown-stained surfaces were quantified using ImageJ software.

Statistical Analysis

Data are reported as mean ± standard error of the mean (SEM). Mann-Whitney tests were performed to compare different conditions using GraphPad Prism 8.0 for Windows. The significance level was set at $p \leq 0,05$.

RESULTS

Pro-inflammatory effects of human calcifications on human monocytes, macrophages and tenocytes

We first observed that synthetic apatite crystals used as control contained larger elements than patients' calcifications. After grinding, we obtained particles with size (1-100 µm length) and morphology (round shape) close to the human calcifications (Figure 1A) [3]. Therefore, we used the grinded synthetic crystals for the following experiments. First, we studied the effects of crystals on IL-1β release by cells of the monocyte/macrophage lineage. We observed that, when cultured with synthetic apatite or human crystals, monocytes and M-CSF or GM-CSF macrophages were able to increase significantly their release of IL-1β (Figure 1B). These increased amounts of IL-1β in the culture supernatants were observed only when the cells had been previously primed overnight with LPS, as observed previously with other microcrystals [7]. Without LPS, there was no detection of IL-1β in the culture medium. At the same crystal concentration (1 mg/ml), synthetic HA stimulation induced significantly higher levels of IL-1β released by M-CSF or GM-CSF macrophages compared to human calcification. In parallel, we observed a significant induced cell death in cultures with crystals compared to control condition. As observed with IL-1β release, cell death was significantly higher with sHA than with patients' calcification but was equivalent between LPS-primed cells and not-primed cells. We also studied the effects of crystal stimulation on tenocyte, the major cell population of the tendon (Figure 1B). We did not observe any significant release of IL-1β in tenocytes supernatants even after priming by LPS, nor any induced cell death, this suggesting that macrophages are the key cells of the inflammation induced by the resorption of calcification.

Pro-inflammatory effects of human calcifications on THP-1 macrophages

To go further in the mechanisms of action of crystals on macrophages, we then used the myeloid cell line THP-1, which was pre-treated with PMA to induce macrophage maturation and priming. This cell line has been previously used to study the inflammatory response to crystals [7].

First and as demonstrated previously with other crystals [11], we observed that secretion of IL-1β was significantly higher when stimulation was performed in FBS-free conditions (Figure 2A). The following

experiments were therefore carried out in FBS-free medium. After crystal stimulation, an increased release of IL-1β was observed after 1 hour and gradually increased within 24 hours (Figure 2B). No IL-1β was detected when human calcifications were incubated alone in the medium without THP-1 cells (Figure 2C). When crystals were applied at increasing concentrations, we observed a dose-dependent increase of IL-1β production for the two types of crystals, with a significantly higher IL-1β release after sHA stimulation at 250 and 500 µg/ml than with patients' apatite (Figure 2D, N=9 patients). Percentage of dead cells also increased with the crystal concentrations and was significantly higher after sHA stimulation at 500 and 1000µg/ml compared to human apatite (Figure 2D). IL-6 and IL-8 release at 6 hours were also quantified by ELISA in THP-1 supernatants: IL-6 was not detectable while IL-8 level was not increased after crystal stimulation (data not shown).

Gene expression of *IL-1β* was increased in THP-1 cells after crystal stimulation as well as *IL-18*, another member of the IL-1 family. We also observed an increased expression of *NF-κB* and *TGFβ1* with both sHA and patients' apatite. In contrast, there was no increase in *IL-1RA* (*Interleukin 1 receptor antagonist)*, *IL-6* and *TNFα* gene expression (Figure 3).

Finally, the release of IL-1β induced by sHA and patients' apatite was significantly reduced by the addition of an inhibitor of NF-κB (BAY-11-7085) as well as an inhibitor of Caspase-1 (Z-YVAD-FMK, Figure 4A). Using western blot analysis, we also found a significant decrease of cleaved IL-1β (mature form of IL-1β) in cell lysates and supernatants although the inhibitor of Caspase 1 only reduced the release of cleaved IL-1β in supernatants but did not reduced the amount of cleaved IL-1β in cell lysates (Figure 4B-C).

Pro-inflammatory effects of human calcifications in an air pouch mouse model

To confirm the inflammatory effect of patients' crystals, we next used the murine air pouch model. In both C57BL/6 and BALB/c mice, injection of patient's crystals or synthetic HA resulted in an infiltration of the membrane with a significant enhanced membrane thickness as early as 6h post-injection (Figure 5A-B-C). Immunohistochemistry showed a significant infiltration of Iba1+ macrophages (Figure 5C-D). Ly6G+ neutrophils were rarely present in the infiltrate as well as CD3+ T lymphocytes and CD45R/B220+ B lymphocytes (data not shown). We also observed the presence of crystals (C in the

215 figure 5C) included within the membrane 6 hours after the injection. While the inflammatory infiltrate
216 was equivalent in the two crystal groups, increase in *IL-1β* gene expression was higher in the synthetic
217 apatite group (figure 5E) and just approached the significance in the human calcification group at the
218 dose of 2 mg/ml (p=0.06). Gene expression of *TNFα* and *IL-6* was not increased in the crystals groups
219 compared to the PBS group (data not shown).

220

221

222

DISCUSSION

Even if the pro-inflammatory effects of the apatite crystals has been yet demonstrated through previous studies using synthetic hydroxyapatite [7-8, 10-11], we demonstrated here the inflammatory effects of crystals extracted from patients suffering from calcific tendinopathies, with their own characteristics in terms of size, shape and protein content. Similarly to MSU and CPPD crystals-induced inflammation, IL-1β is the central cytokine in the process and its release depends on NLRP3 inflammasome activation. In gout and acute CPP crystal arthritis, the crystals taken up by macrophages first enhance pro-IL-1β expression during the priming phase and then promote the assembly and activation of the NLRP3 inflammasome. The NLRP3 inflammasomes are formed by the recruitment of the adaptor protein ASC and subsequent recruitment of caspase-1 [14-15]. Caspase-1 activates the pro-inflammatory cytokines IL-1β and IL-18 by cleaving their respective precursor proteins, pro-IL-1β and pro-IL-18. Then, IL-1β drives further inflammation by promoting (1) cytokine and chemokine production, (2) endothelial cell activation, (3) PGE2 production and (4) neutrophil recruitment [14].

We showed *in vitro* that human calcifications were able to induce the release of IL-1β by human monocytes, macrophages and the myeloid cell line THP-1 but not tenocytes. As observed with other microcrystals [7], cell priming using LPS or PMA was necessary to provide a first signal for IL-1β production. Following this priming phase, we also observed that patient's crystals enhanced mRNA expression of *IL-1β*, as well as *IL-18*, *NF-κB* and *TGFβ1* (Figure 3). Crystals from 9 different patients induced IL-1β release from THP-1 cells in a time and dose-dependent manner but IL-6 was not detectable in culture supernatants at 6h of stimulation probably because it is produced later [11]. Moreover, inhibition of NF-κB significantly reduced the production and release of the matured form of IL-1β (17kDa, Figure 4B and C). The inhibition of caspase-1 similarly reduced the release of matured IL-1 β into the culture supernatant but did not prevent the maturation of this cytokine in cell lysates (Figure 4B and C). Our current hypothesis is that other caspases such as caspase-8 could be implicated in IL-1β maturation while caspase-1 would be necessary for IL-1β release through gasdermin D maturation, pore formation and pyroptosis [16].

In vivo, human calcifications were able to induce a thickening of air pouch membranes with an infiltrate composed mainly of macrophages, showing once again the contribution of these cells in the response to crystal stimulation. However, the increased expression of *IL-1β* in the membranes was higher with synthetic apatite suggesting a lower inflammatory activity of patients' crystals in these experiments. This lower inflammatory potential of human calcifications compared to synthetic apatite was also observed when crystals were incubated with human macrophages. This difference could first be explained by a different size and shape of human and synthetic crystals. Indeed, small and needle-shaped crystals were more likely to produce an IL-1β mediated inflammatory response compared to large and spherical crystals [8,17]. In our samples, particles size varied from 3 to 300 µm [3], with a spherical morphology. Although the particles size and shape were grossly similar between patients and grinded synthetic HA, we cannot exclude that particles heterogeneity would lead to variable pro-inflammatory effects on cells. We can also hypothesize that only a portion of the particles was involved in the induction of IL-1β secretion and could vary between patients depending on the disparity in crystal size within the samples.

Secondly, protein present on crystals may also have a role. It has been shown that MSU crystals can be coated by several proteins (albumin, ovalbumin, immunoglobulin (Ig), fibrinogen, fibronectin, lysozyme, apolipoproteins and high and low density lipoproteins (HDL and LDL)) [18-22], and that these adsorbed proteins could influence the inflammatory properties of MSU crystals. For example, MSU crystals isolated from sites of gouty inflammation are coated with immunoglobulins (mainly IgG), whose surface concentrations decline as inflammation resolves (inversely correlating with a rise in apolipoprotein B surface coating), suggesting a regulatory role of these elements in acute gout attack [23-24]. The effects of protein coating on CPPD crystal-induced inflammation have also been recently studied [25]. As observed in our experiments, when m-CPPD (monoclinic calcium pyrophosphate dihydrate) crystals were incubated with FBS, the release of IL-1β by THP-1 was significantly decreased. Otherwise, BSA-coated crystals were less likely able to induce IL-1β release. The modulation of crystal-induced inflammation by protein adsorption was the result of interferences on crystal/cell membrane interactions. By proteomic analysis, we have found in a previous study similarities with proteins that can be coated on MSU (fibronectin, albumin, apolipoproteins, fibrinogen) [3]. In addition, several proteins implicated in the regulation of inflammation and immune reactions (Osteopontin, Osteoprotegerin or Periostin) were previously found associated with patients' crystals [3]. However, the influence of

proteins absorbed on human apatite crystals on their inflammatory properties has not been studied yet and may be the purpose of future studies.

CONCLUSION

As synthetic hydroxyapatite, human calcifications were able to induce an inflammatory response resulting in the production of IL-1β after NF-κB activation and through NLRP3 inflammasome. In some experiments, IL-1β induction was lower with human calcifications compared to synthetic apatite. Differences in size, shape and protein content may explain this observation. Further studies would be necessary to explore the potential role of protein in the regulation of the inflammation induced by the crystals.

LIST OF ABBREVIATIONS

CAL: human calcification

CPPD: calcium pyrophosphate dihydrate

Ct: cycle threshold

CT: control group

FBS: fetal bovine serum

GAPDH: Glyceraldehyde 3-phosphate dehydrogenase

GM-CSF: Granulocyte-Macrophage Colony Stimulating Factor

H&E: Hematoxylin and eosin

HPRT: hypoxanthine-guanine phosphoribosyl transferase

IFN-γ: Interferon gamma

IHC: immunohistochemistry

IL: interleukin

IL1RA: Interleukin 1 receptor antagonist

LPS: lipopolysaccharide

M-CSF: Macrophage Colony Stimulating Factor

MSU: monosodium urate

NF-κB: Nuclear factor-kappa B

NLRP3: NOD-like receptor family, pyrin domain containing 3

PBS: Phosphate-buffered saline

PCR: polymerase chain reaction

PMA: Phorbol 12-myristate 13-acetate

RNA: ribonucleic acid

SEM: standard error of the mean

sHA: synthetic hydroxyapatite

TGF-β: Transforming growth factor beta

TNF: Tumor necrosis factor

DECLARATIONS

Ethics approval : Animal experiments were carried out in accordance with institutional guidelines and were approved by the French ethical committee CEEA Pays de la Loire and by local veterinary services (Approval number APAFIS#4969-2016041411376797v3).

Consent for publication: Not applicable

Availability of data and materials: The datasets used and/or analyzed during the current study are available from the corresponding author on reasonable request.

Competing interests: the authors have no conflicts of interest to declare.

Funding: The study was performed with the financial support of the “Fondation Arthritis Recherche et Rhumatismes” and the “French Society for Rheumatology”.

Authors’ contributions: JH, JDL, RB, CC, FB and CDL have contributed to the acquisition and analysis of data. JH, BLG, FB and CDL have contributed to the conception, the design of the work and have drafted the manuscript. All authors read and approved the final manuscript.

Acknowledgements: not applicable

REFERENCES

1/ Darrieutort-Laffite C, Blanchard F, Le Goff B. Calcific tendonitis of the rotator cuff: From formation to resorption. Joint Bone Spine. 2018 Dec;85(6):687-692. doi:10.1016/ j.jbspin.2017.10.004. Epub 2017 Nov 28.

2/ Uhthoff HK, Loehr JW. Calcific tendinopathy of the rotator cuff: pathogenesis, diagnosis and management. J Am Acad Orthop Surg 1997 Jul;5(4):183-191. doi: 10.5435/00124635-199707000-00001.

3/ Darrieutort-Laffite C, Arnolfo P, Garraud T, Adrait A, Couté Y, Louarn G, et al. Rotator Cuff Tenocytes Differentiate into Hypertrophic Chondrocyte-Like Cells to Produce Calcium Deposits in an Alkaline Phosphatase-Dependent Manner. J Clin Med. 2019 Sep 26;8(10):1544. doi: 10.3390/jcm8101544.

4/ Uhthoff HK. Calcifying tendinitis, an active cell-mediated calcification. Virchows Arch A Pathol Anat Histol 1975;366:51–8. doi: 10.1007/BF00438677.

5/ Archer RS, Bayley JI, Archer CW, Ali SY. Cell and matrix changes associated with pathological calcification of the human rotator cuff tendons. J Anat 1993;182:1–11.

6/ Nakase T, Takeuchi E, Sugamoto K, Kaneko M, Tomita T, Myoui A, et al. Involvement of multinucleated giant cells synthesizing cathepsin K in calcified tendinitis of the rotator cuff tendons. Rheumatology (Oxford) 2000;39:1074–7. doi: 10.1093/rheumatology/ 39.10.1074.

7/ Pazár B, Ea HK, Narayan S, Kolly K, Bagnoud N, Chobaz V, et al. Basic calcium phosphate crystals induce monocyte/macrophage IL-1secretion through the NLRP3 inflammasome in vitro. J Immunol 2011;186:2495–502. doi: 10.4049/jimmunol.1001284. Epub 2011 Jan 14.

8/ Jin C, Frayssinet P, Pelker R, Cwirka D, Hu B, Vignery A, et al. NLRP3 inflammasome plays a critical role in the pathogenesis of hydroxyapatite-associated arthropathy. Proc Natl Acad Sci U S A 2011;108:14867–72. doi: 10.1073/pnas.1111101108. Epub 2011 Aug 19.

9/ Kowanko IC, Gordon TP, Rozenbilds MA, Brooks PM, Roberts-Thomson PJ. The subcutaneous air pouch model of synovium and the inflammatory response to heat aggregated gammaglobulin. Agents Actions 1986;18:421–8. doi: 10.1007/BF01965007.

10/ Prudhommeaux F, Schiltz C, Lioté F, Hina A, Champy R, Bucki B, et al. Variation in the inflammatory properties of basic calcium phosphate crystals according to crystal type. Arthritis Rheum 1996;39:1319–26. doi: 10.1002/art.1780390809.

11/ Campillo-Gimenez L, Renaudin F, Jalabert M, Gras P, Gosset M, Rey C, et al. Inflammatory Potential of Four Different Phases of Calcium Pyrophosphate Relies on NF-kappaB Activation and MAPK Pathways. Front Immunol. 2018 Oct 9;9:2248. doi: 10.3389/fimmu.2018.02248. eCollection 2018.

12/ Nakayama M. Macrophage Recognition of Crystals and Nanoparticles. Front Immunol. 2018 Jan 29;9:103. doi: 10.3389/fimmu.2018.00103. eCollection 2018.

13/ Grases F, Muntaner-Gimbernat L, Vilchez-Mira M, et al. Characterization of deposits in patients with calcific tendinopathy of the supraspinatus. Role of phytate and osteopontin. J Orthop Res. 2015;33(4):475-82.

14/ McCarthy GM, Dunne A. Calcium crystal deposition diseases - beyond gout. Nat Rev Rheumatol. 2018 Oct;14(10):592-602. doi: 10.1038/s41584-018-0078-5.

15/ So AK, Martinon F. Inflammation in gout: mechanisms and therapeutic targets. Nat Rev Rheumatol. 2017 Nov;13(11):639-647. doi: 10.1038/nrrheum.2017.155. Epub 2017 Sep 28.

16/ Schneider KS, Groß CJ, Dreier RF, Saller BS, Mishra R, Gorka O, et al. The Inflammasome Drives GSDMD-Independent Secondary Pyroptosis and IL-1 Release in the Absence of Caspase-1 Protease Activity. Cell Rep. 2017 Dec 26;21(13):3846-3859. doi: 10.1016/j.celrep.2017.12.018.

17/ Lebre F, Sridharan R, Sawkins MJ, Kelly DJ, O'Brien FJ, Lavelle EC. The shape and size of hydroxyapatite particles dictate inflammatory responses following implantation. Sci Rep. 2017 Jun 7;7(1):2922. doi: 10.1038/s41598-017-03086-0.

18/ Kozin F, McCarty DJ. Protein adsorption to monosodium urate, calcium pyrophosphate dihydrate, and silica crystals: relationship to the pathogenesis of crystal-induced inflammation. Arthritis Rheum. 1976 May-Jun;19 Suppl 3:433-8. doi: 10.1002/1529-0131(197605/06)19:3+<433::aid-art1780190718>3.0.co;2-u.

386 19/ Kozin F, McCarty DJ. Protein binding to monosodium urate monohydrate, calcium pyrophosphate
387 dihydrate, and silicon dioxide crystals. I. Physical characteristics. J Lab Clin Med. 1977 Jun;89(6):1314-
388 25.

389 20/ Terkeltaub R, Martin J, Curtiss LK, Ginsberg MH. Apolipoprotein B mediates the capacity of low
390 density lipoprotein to suppress neutrophil stimulation by particulates. J Biol Chem. 1986 Nov
391 25;261(33):15662-7.

392 21/ Abramson S, Hoffstein ST, Weissmann G. Superoxide anion generation by human neutrophils
393 exposed to monosodium urate. Arthritis Rheum. 1982 Feb;25(2):174-80. doi:10.1002/art.1780250210.

394 22/ Scanu A, Luisetto R, Oliviero F, Gruaz L, Sfriso P, Burger D, et al. High-density lipoproteins inhibit
395 urate crystal-induced inflammation in mice. Ann Rheum Dis. 2015 Mar;74(3):587-94. doi:
396 10.1136/annrheumdis-2013-203803. Epub 2013 Dec 10.

397 23/ Ortiz-Bravo E, Sieck MS, Schumacher HR Jr. Changes in the proteins coating monosodium urate
398 crystals during active and subsiding inflammation. Immunogold studies of synovial fluid from patients
399 with gout and of fluid obtained using the rat subcutaneous air pouch model. Arthritis Rheum. 1993;
400 36(9):1274–85. doi: 10.1002/art.1780360912.

401 24/ Cherian PV, Schumacher HR Jr. Immunochemical and ultrastructural characterization of serum
402 proteins associated with monosodium urate crystals (MSU) in synovial fluid cells from patients with gout.
403 doi: 10.3109/01913128609032219. Ultrastruct Pathol. 1986; 10(3):209–19.

404 25/ Renaudin F, Sarda S, Campillo-Gimenez L, Séverac C, Léger T, Charvillat C, et al. Adsorption of
405 Proteins on m-CPPD and Urate Crystals Inhibits Crystal-induced Cell Responses: Study on Albumin-
406 crystal Interaction. J Funct Biomater. 2019 Apr 25;10(2):18. doi: 10.3390/jfb10020018.
407

TABLES AND FIGURES

FIGURE 1 | A: Representative images of calcific powders obtained by Scanning Electron Microscopy. A1: Human sample collected after a percutaneous needle lavage under ultrasound. A2 and A3: Synthetic hydroxyapatite before and after grinding respectively. B: IL-1β release after 6h stimulation of CD14+ monocytes, MCSF-Macrophages, GM-CSF/IFNγ-Macrophages and tenocytes by crystals (1mg/ml) and parallel cell death rate. sHA= synthetic hydroxyapatite, CAL = human calcification CT= control group without crystal; LPS= lipopolysaccharide; ND= not detectable. n=3. * p≤ 0,05

FIGURE 2 | IL-1β production by THP-1 cells after crystal stimulation. A: Release of IL-1β by THP-1 cells cultured during 6 hours with crystals (1mg/ml) in media with or without 10% fetal bovine serum (FBS) (n=3). B: Kinetic of IL-1β production by THP-1 cells cultured with a patient's calcification (CAL, 1mg/ml), synthetic hydroxyapatite (sHA, 1 mg/ml) or without crystal (CT) (n=3). C: IL-1β release in cultures containing only crystals compared to THP-1 cells after crystal stimulation (N=3 patients). D: IL-1β quantification in supernatants of THP-1 after 6 hours of crystal stimulation with increasing concentrations of calcifications of 9 different patients (N=9). sHA= synthetic hydroxyapatite; CAL= human calcification; CT = control condition without crystals. *p ≤ 0.05.

FIGURE 3 | THP-1 gene expression after 6h stimulation by crystals (synthetic hydroxyapatite (sHA) or human calcification (CAL) at 1 mg/mL). Gene expression is expressed in relative expression ($2^{-\Delta Ct}$) with *HPRT* gene used as reference. CT = control condition without crystal. *p ≤ 0,05 (n=3).

FIGURE 4 | Effects of a NF-κB inhibitor and a caspase-1 inhibitor on the secretion of IL-1β by THP-1 macrophages. A: quantification of IL-1β released into the medium after 6h stimulation by crystals (1mg/ml) in presence or absence of a NF-κB inhibitor (BAY-11-7085, 10µM) or a caspase-1 inhibitor (Z-YVAD-FMK, 10 µM) (n=3). B and C: Effects of crystals and inhibitors on NLRP3 and IL-1β assessed by Western Blot on cell lysates and supernatants (SN). One representative patient out of 3 is presented in B and quantification of cleaved-IL-1β in cell lysates and supernatant is presented in C (N=3 patients),

435 with GAPDH used as an invariant protein. sHA= synthetic hydroxyapatite; CAL= human calcification;
436 CT = control condition without crystals. *p ≤ 0.05

437

438 **FIGURE 5** | *In vivo* effects of human calcifications in a mouse air pouch model. A: Assessment of
439 membrane thickness (H&E staining) 6 and 24 hours after crystals injection (1mg/ml) in C57BL/6 mice
440 (N=3-5/group). B: Assessment of membrane thickness 6 and 24 hours after crystals injection (1mg/ml)
441 in BALB/c mice (N=4-5/group). C: Representative images of H&E and Iba1 staining 6 hours after the
442 injection for each group in C57BL/6 mice. D: Quantification of the Iba1+ macrophage infiltration 6 hours
443 after the injection in C57BL/6 mice (N=3-5/group). Results are expressed as Iba1+ stained surface (%)
444 as assessed using ImageJ software. E: *IL-1β* gene expression in air pouch membranes 6 hours after
445 the injection of crystals (1 or 2 mg/ml as indicated) (N=5/group). Gene expression is expressed in
446 relative expression ($2^{-\Delta Ct}$) with *HPRT* gene used as reference. sHA=synthetic apatite; CAL=human
447 calcification; H&E= Hematoxylin and eosin. C=crystals.*p<0.05.

448

449 **Supplementary table 1** | Primers used for quantitative Polymerase Chain Reaction.

Figures

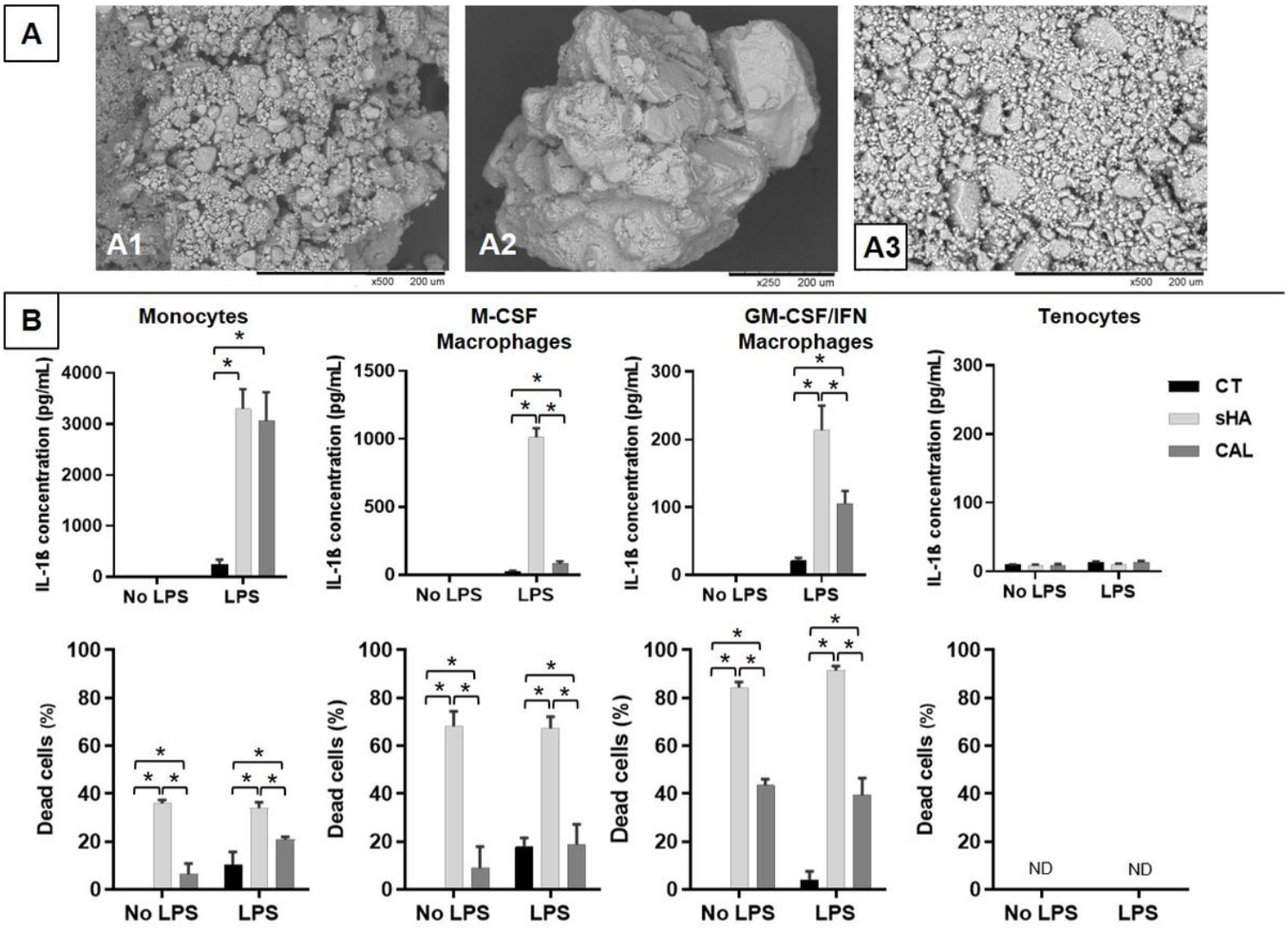

Figure 1

A: Representative images of calcific powders obtained by Scanning Electron Microscopy. A1: Human sample collected after a percutaneous needle lavage under ultrasound. A2 and A3: Synthetic hydroxyapatite before and after grinding respectively. B: IL-1β release after 6h stimulation of CD14+ monocytes, MCSF-Macrophages, GM-CSF/IFNγ-Macrophages and tenocytes by crystals (1mg/ml) and parallel cell death rate. sHA= synthetic hydroxyapatite, CAL = human calcification CT= control group without crystal; LPS= lipopolysaccharide; ND= not detectable. n=3. * p≤ 0,05

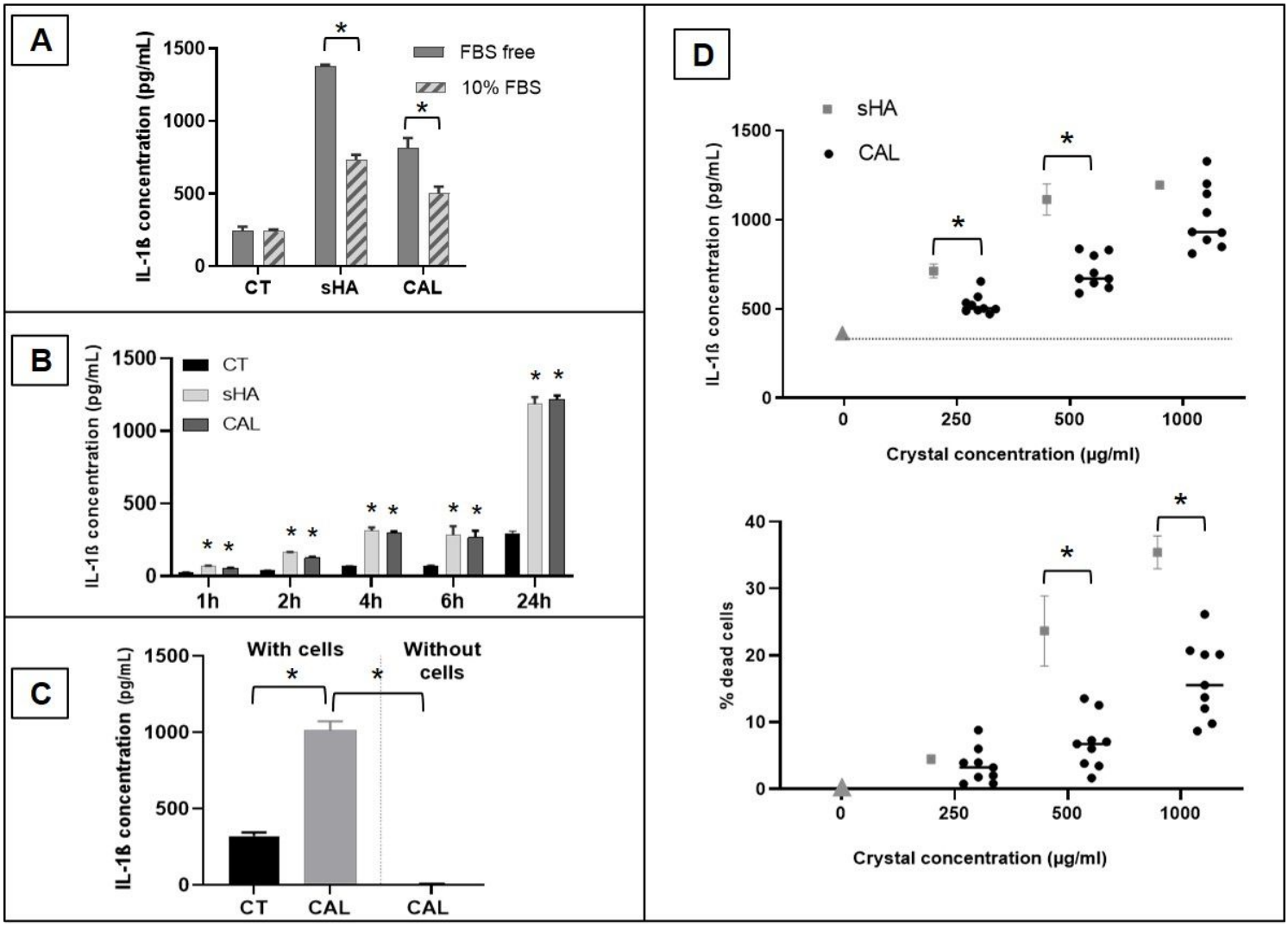

Figure 2

IL-1β production by THP-1 cells after crystal stimulation. A: Release of IL-1β by THP-1 cells cultured during 6 hours with crystals (1mg/ml) in media with or without 10% fetal bovine serum (FBS) (n=3). B: Kinetic of IL-1β production by THP-1 cells cultured with a patient's calcification (CAL, 1mg/ml), synthetic hydroxyapatite (sHA, 1 mg/ml) or without crystal (CT) (n=3). C: IL-1β release in cultures containing only crystals compared to THP-1 cells after crystal stimulation (N=3 patients). D: IL-1β quantification in supernatants of THP-1 after 6 hours of crystal stimulation with increasing concentrations of calcifications of 9 different patients (N=9). sHA= synthetic hydroxyapatite; CAL= human calcification; CT = control condition without crystals. *$p \leq 0.05$.

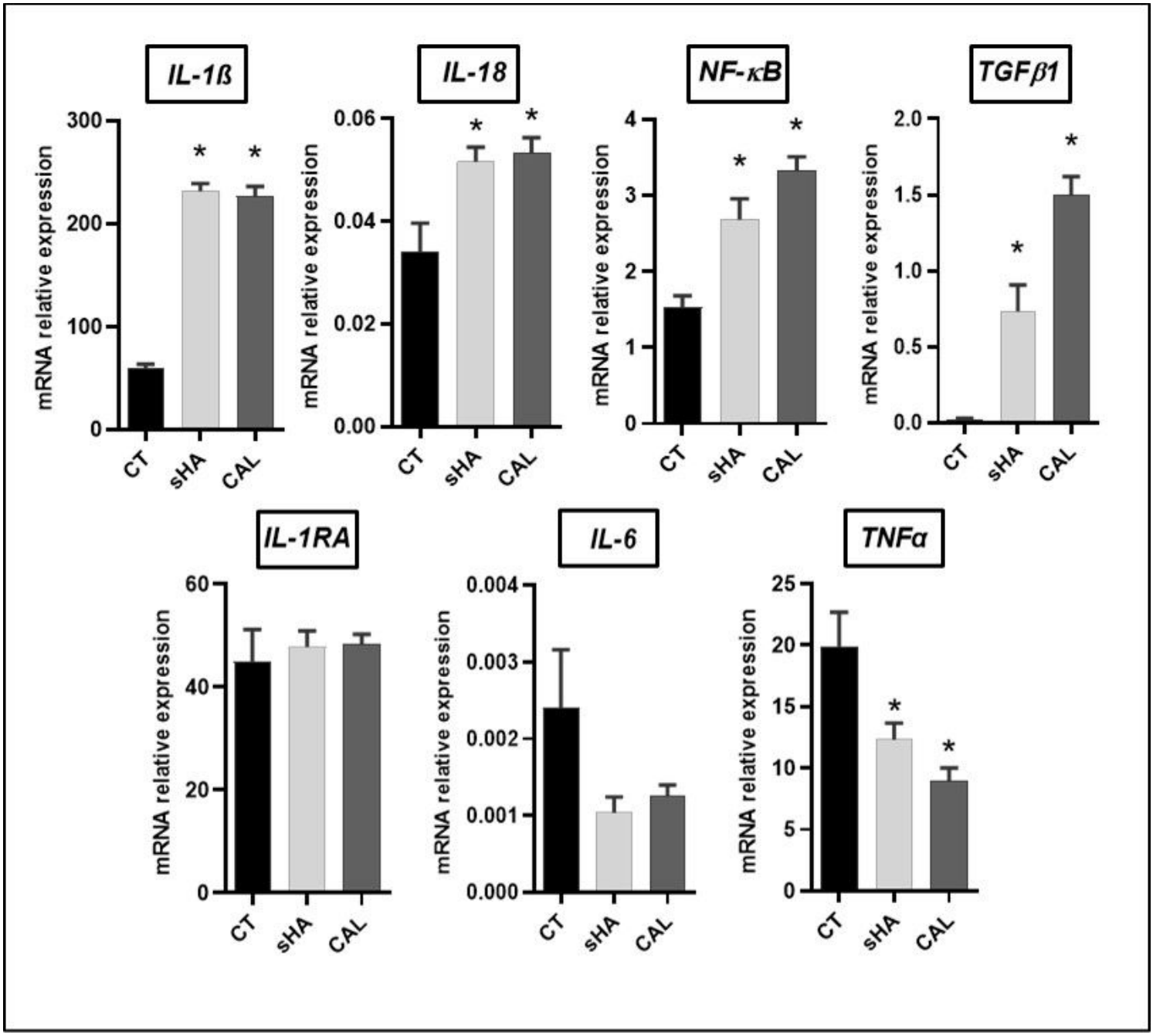

Figure 3

THP-1 gene expression after 6h stimulation by crystals (synthetic hydroxyapatite (sHA) or human calcification (CAL) at 1 mg/mL). Gene expression is expressed in relative expression (2-ΔCt) with HPRT gene used as reference. CT = control condition without crystal. *p ≤ 0,05 (n=3).

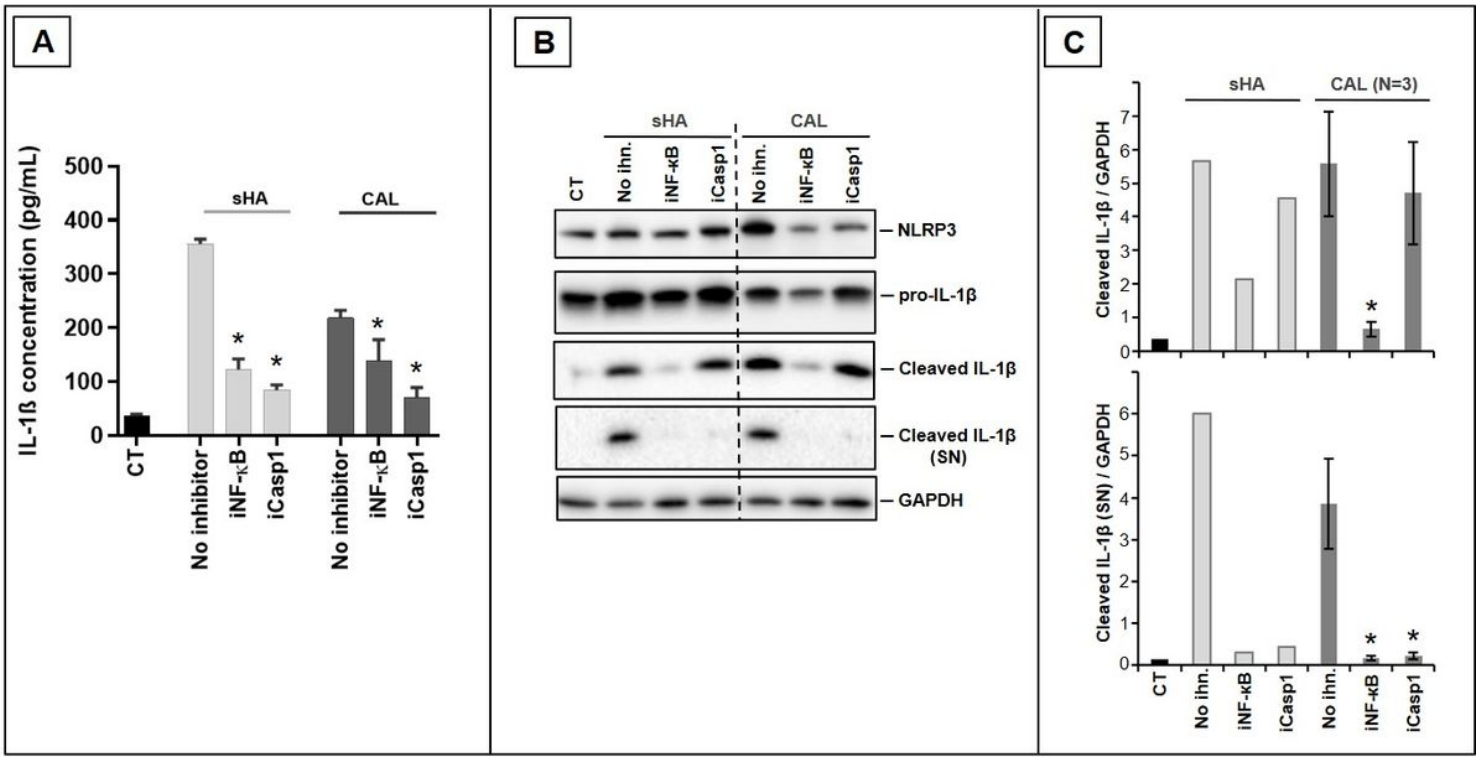

Figure 4

Effects of a NF-κB inhibitor and a caspase-1 inhibitor on the secretion of IL-1β by THP-1 macrophages. A: quantification of IL-1β released into the medium after 6h stimulation by crystals (1mg/ml) in presence or absence of a NF-κB inhibitor (BAY-11-7085, 10µM) or a caspase-1 inhibitor (Z-YVAD-FMK, 10 µM) (n=3). B and C: Effects of crystals and inhibitors on NLRP3 and IL-1β assessed by Western Blot on cell lysates and supernatants (SN). One representative patient out of 3 is presented in B and quantification of cleaved-IL-1β in cell lysates and supernatant is presented in C (N=3 patients), with GAPDH used as an invariant protein. sHA= synthetic hydroxyapatite; CAL= human calcification; CT = control condition without crystals. *$p \leq 0.05$

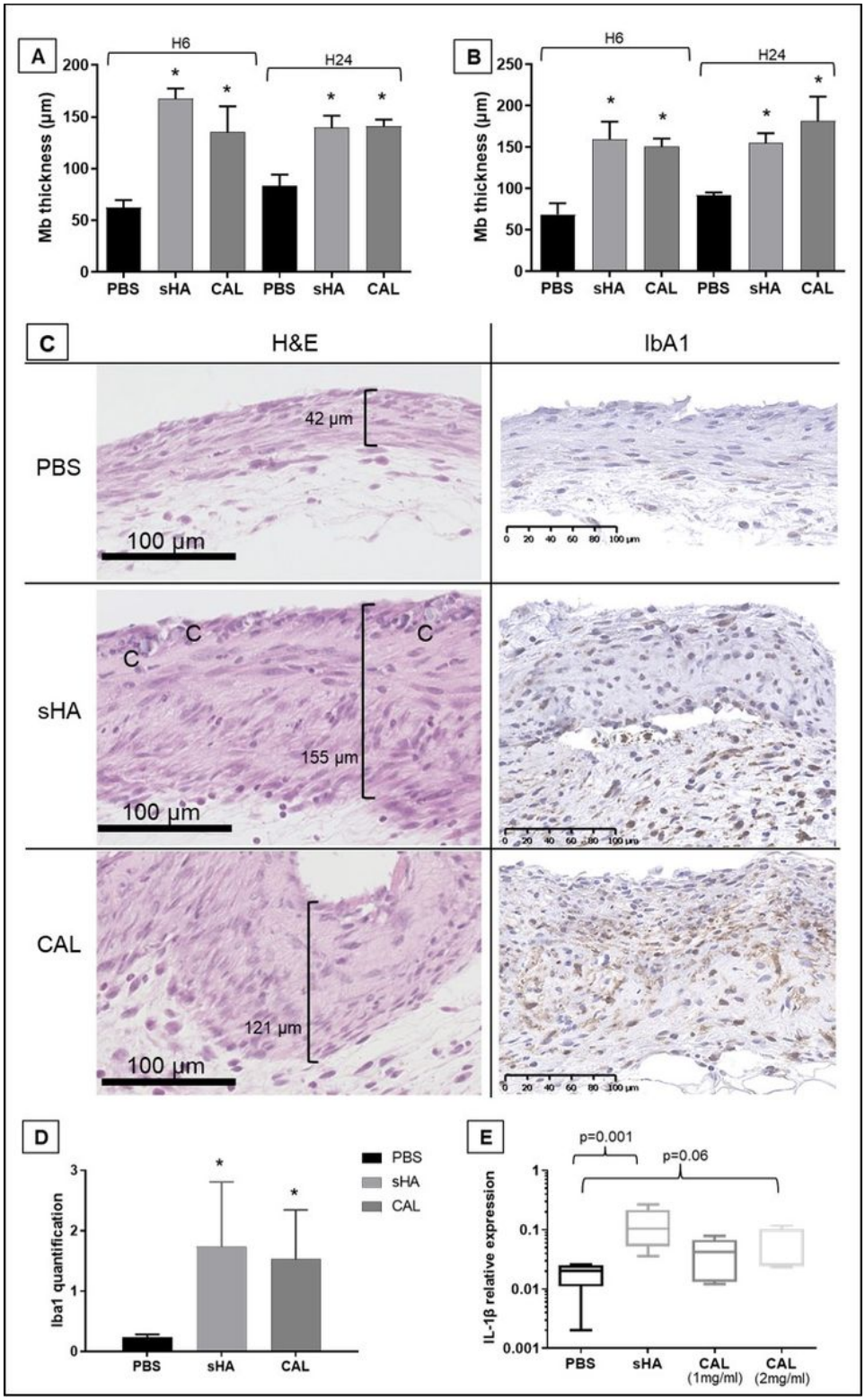

Figure 5

In vivo effects of human calcifications in a mouse air pouch model. A: Assessment of membrane thickness (H&E staining) 6 and 24 hours after crystals injection (1mg/ml) in C57BL/6 mice (N=3-5/group). B: Assessment of membrane thickness 6 and 24 hours after crystals injection (1mg/ml) in BALB/c mice (N=4-5/group). C: Representative images of H&E and Iba1 staining 6 hours after the injection for each group in C57BL/6 mice. D: Quantification of the Iba1+ macrophage infiltration 6 hours

after the injection in C57BL/6 mice (N=3-5/group). Results are expressed as Iba1+ stained surface (%) as assessed using ImageJ software. E: IL-1β gene expression in air pouch membranes 6 hours after the injection of crystals (1 or 2 mg/ml as indicated) (N=5/group). Gene expression is expressed in relative expression (2-ΔCt) with HPRT gene used as reference. sHA=synthetic apatite; CAL=human calcification; H&E= Hematoxylin and eosin. C=crystals.*p<0.05.

Supplementary Files

This is a list of supplementary files associated with this preprint. Click to download.

- Supplementarytable1.pdf